Received: 12 January 2023 | Revised: 13 April 2023 | Accepted: 4 May 2023

https://doi.org/10.1016/j.jtha.2023.05.004

ORIGINAL ARTICLE

Bioactive surface coating for preventing mechanical heart valve thrombosis

Patrizio Lancellotti[1] | Abdelhafid Aqil[2] | Lucia Musumeci[1] | Nicolas Jacques[1] | Bartosz Ditkowski[1] | Margaux Debuisson[1] | Marc Thiry[3] | Julien Dupont[4] | Alexandra Gougnard[4] | Charlotte Sandersen[4] | Jean-Paul Cheramy-Bien[5,6] | Natzi Sakalihasan[5,6] | Alain Nchimi[1] | Christophe Detrembleur[2] | Christine Jérôme[2] | Cécile Oury[1]

[1]Laboratory of Cardiology, GIGA Institute, and Department of Cardiology, Centre Hospitalier Universitaire of Liège, University of Liège Hospital, Liège, Belgium

[2]Center for Education and Research on Macromolecules, CESAM Research Unit, University of Liège, Liège, Belgium

[3]Laboratory of Cellular and Tissular Biology, GIGA-Neurosciences, Cell Biology, University of Liège, Liège, Belgium

[4]Department of Clinical Sciences, Faculty of Veterinary Medicine, University of Liège, Liège, Belgium

[5]Department of Cardiovascular and Thoracic Surgery, Centre Hospitalier Universitaire of Liège, University of Liège, Liège, Belgium

[6]Surgical Research Center, GIGA-Cardiovascular Science Unit, University of Liège, Liège, Belgium

Correspondence
Cécile Oury, Laboratory of Cardiology, GIGA-Cardiovascular Sciences Unit, University of Liège, Avenue de l'Hôpital 1, B-4000 Liège, Belgium.
Email: cecile.oury@uliege.be

Funding information
This work was supported by the European Research Council, Consolidator grant (PV-COAT grant number 647197). C.O. is Research Director at the Belgium National Funds for Scientific Research (F.R.S.-FNRS).

Abstract

Background: Prosthetic heart valves are the only treatment for most patients with severe valvular heart disease. Mechanical valves, made of metallic components, are the most long-lasting type of replacement valves. However, they are prone to thrombosis and require permanent anticoagulation and monitoring, which leads to higher risk of bleeding and impacts the patient's quality of life.

Objectives: To develop a bioactive coating for mechanical valves with the aim to prevent thrombosis and improve patient outcomes.

Methods: We used a catechol-based approach to produce a drug-releasing multilayer coating adherent to mechanical valves. The hemodynamic performance of coated Open Pivot valves was verified in a heart model tester, and coating durability in the long term was assessed in a durability tester producing accelerated cardiac cycles. Coating antithrombotic activity was evaluated *in vitro* with human plasma or whole blood under static and flow conditions and *in vivo* after surgical valve implantation in a pig's thoracic aorta.

Results: We developed an antithrombotic coating consisting of ticagrelor- and minocycline-releasing cross-linked nanogels covalently linked to polyethylene glycol. We demonstrated the hydrodynamic performance, durability, and hemocompatibility of coated valves. The coating did not increase the contact phase activation of coagulation, and it prevented plasma protein adsorption, platelet adhesion, and thrombus formation. Implantation of coated valves in nonanticoagulated pigs for 1 month efficiently reduced valve thrombosis compared with noncoated valves.

Conclusion: Our coating efficiently inhibited mechanical valve thrombosis, which might solve the issues of anticoagulant use in patients and the number of revision surgeries due to valve thrombosis despite anticoagulation.

Manuscript handled by: Roger Preston

Final decision: Roger Preston, 04 May 2023

KEYWORDS
animal experimentation, heart valves, platelet aggregation inhibitors, prostheses and implants, thrombosis

1 | INTRODUCTION

Heart valve diseases are a growing public health concern worldwide. Heart valve replacements of diseased cardiac valves by prostheses (prosthetic valves [PVs]) is common and often lifesaving for patients with significant valvular lesions, stenosis, or regurgitation [1,2]. PVs are currently among the most widely used cardiovascular devices [3]. Approximately 300 000 PV implantations are performed every year worldwide; the total number of valve replacements is projected to be 850 000 per year by 2050. Two types of PVs are in use today to fulfill this growing demand, mechanical and bioprosthetic valves, each with its inherent assets and drawbacks [4]. Mechanical PVs, made from synthetic materials and with unnatural hemodynamics, are prone to thrombus formation without anticoagulation therapy, which inevitably increases the bleeding risk [5]. To date, issues related to the need for lifelong anticoagulation with mechanical valves have not been resolved. Vitamin K antagonist remains the only option, which necessitates constant monitoring with a huge impact on the patient's quality of life. The management of bridging anticoagulation before and after invasive procedures is controversial, with excess risk of complications. The advantage of biological PVs is their lower thrombotic risk compared with that with mechanical ones, which typically does not necessitate lifelong oral anticoagulation. The anticoagulation requirement has been the key reason for the continuous decline of mechanical valve use in patients aged 50 to 70 years over the past decades in certain geographic areas [6,7]. Major advances in transcatheter valve replacement approaches might have contributed to this trend [8–11]. However, bioprosthetic valves are subject to progressive structural valve deterioration, which hampers their performance beyond 10 to 20 years [12], and leaflet thrombosis is less negligible than initially thought [13–15]. Therefore, there is a need for innovation in durable valves that would require minimal anticoagulation.

We have developed a new polymeric bioactive coating for PVs endowed with antithrombotic properties. We used a catechol-based approach to produce a multilayer nanogel (NG) coating that adheres to the entire valve prosthesis, ie, its metallic (pyrolytic carbon and titanium) and polymeric (polyethylene terephthalate) constituents. The desired biological activity of the coating was obtained by loading the NGs with ticagrelor and by covalent binding of polyethylene glycol (PEG) on top of the multilayer NG assembly through thiol/quinone reactions. We demonstrated the hemodynamic performance, hemocompatibility, and thromboresistance of the bioactive surface–coated PV *in vitro* and *in vivo* in a nonanticoagulated pig model of valve implantation.

Essentials

- Mechanical valves are prone to thrombosis and require permanent anticoagulation and monitoring.
- There is a need for innovation in durable valves with minimal anticoagulation requirement.
- We report the development and antithrombotic efficacy of a unique bioactive coating.
- Coating reduced valve thrombosis in nonanticoagulated pigs and might improve valve durability.

2 | METHODS

2.1 | Materials

Mechanical valves (19-mm Open Pivot standard aortic heart valve) were obtained from Medtronic. Minocycline was purchased from Sigma-Aldrich. The antiplatelet drug ticagrelor was from Cayman Chemicals. Sodium citrate vacutainer blood collection tubes (3.2% sodium citrate) were from BD Biosciences. *Staphylococcus aureus* was purchased from ATCC (#25904). Tryptic Soy Broth and agar powder were from Sigma-Aldrich. 3,4-dihydroxy-L-phenylalanine (DOPA) methyl ester hydrochloride was synthesized by reacting SOCl2 with DOPA in dry CH3OH according to a previously described procedure [16]. PEG PEG2 (methoxy-PEG-$[CH_2]_2$-SH; molecular weight [M_w], 2000 g/mol) and PEG5 (methoxy-PEG-$[CH_2]_2$-SH; M_w, 5000 g/mol), dopamine hydrochloride, Tris(hydroxymethyl)aminomethane, sodium chloride, and poly(allylamine) hydrochloride (PAH; M_w, 15 000 g/mol) of the highest grade were purchased from Sigma-Aldrich.

2.2 | NG formation

N-methacryloyl 3,4-dihydroxy-L-phenylalanine methyl ester (mDOPA), synthetized according to available methods [17], was polymerized into P(mDOPA) [18] and was used to prepare NGs, as described in Supplementary Methods [19]. Drug-loaded NGs were prepared as follows: oxidized Pox(mDOPA) (0.5 mg/mL) was solubilized in the presence of 1 mL of ticagrelor solution (56, 112 or 256 μg/mL in dimethylsulfoxide) or minocycline (0.5 mg/mL in water). After 1 hour at 6 °C, an aqueous solution of PAH (0.5 mL; 0.5 g/L) at pH 10

was slowly added to the mixture under vigorous stirring. The solution was left to react for one night at 6 °C under vigorous stirring.

2.3 | Coating process

Synthetic polymers (medical-grade polyurethane Carbothane 3575A from Lubrizol, cell culture grade polystyrene CELLSTAR from Greiner Bio-One) or PVs were modified by using a dip coating process in successive coating solutions. Surfaces were rinsed with ultrapure water after each layer. The first anchored layer was created with the use of a dopamine solution (0.125 mg/mL in 10-mM Tris-HCl, pH 8.5) followed by oxidation-induced polymerization (slow addition of NaOH 0.1M) for 3 hours, visualized by color changes to dark brown. The coated surfaces were then processed for PAH ad-layer formation by immersion in an aqueous solution of PAH (pH, >10) for 1 hour. Multiple layers of NGs were added by alternate dipping in NG solutions (6 hours per layer) and PAH solution (1 hour). PEG grafting on the NG coating was then performed by dipping the coated materials in a solution of thiol end-functionalized PEG (5 mg/mL in degassed Tris buffer pH 8.0).

2.4 | Coating uniformity and integrity testing

Coating uniformity on mechanical valves and its integrity after durability testing and sterilization were assessed by time-of-flight secondary ion mass spectrometry (ToF-SIMS) (ToF-SIMS V; IONTOF) analysis of at least 10 random zones on the valve surface, as described in Supplementary Methods.

2.5 | Ticagrelor release assay and content analysis

Polyurethane discs 8 mm in diameter were coated with 1 or multiple layers of NGs loaded with ticagrelor or not. Drug release was analyzed during 240 hours in a solution of phosphate-buffered saline containing 40% glycerol and 10% methanol (v/v) (dissolution medium). In brief, discs were placed in a test tube with 1 mL of dissolution medium and incubated at room temperature without agitation for up to 240 hours. At indicated time points, the medium was aspirated and stored at −20 °C for later measurements, and a fresh solution was added to the test tube for another period. Aliquots of 200 μL were transferred to a 96-well polystyrene plate, and the absorbance of ticagrelor was measured at 299 nm in a spectrophotometer. Quantity of ticagrelor was determined by using a calibration curve with ticagrelor standard. Ticagrelor content in coated discs was determined by high-performance liquid chromatography on a Waters Acquity ultra pressure liquid chromatography System consisting of a quaternary solvent delivery system, an injector with adjustable injection volume, a temperature-controlled autosampler, a column thermostat, and a photo diode array detector. The assay method was developed according to the ticagrelor monograph (European Pharmacopeia 10.4). Briefly, the analytical column was an XBridge Phenyl, 150 × 4.6 mm, 3μm (Waters) with the guard column Security Guard Phenyl, 3 × 4 mm (Phenomenex). An injection volume of 50 μL was used at a flow rate of 1.0 mL/min at 40 °C (column temperature). Mobile phase A was phosphate buffer (pH 3.0)–water–acetonitrile (1:89:10 v/v/v). Mobile phase B was phosphate buffer (pH 3.0)–water–acetonitrile (1:29:70 v/v/v). Detection wavelength was 300 nm (Supplementary Figure S1).

2.6 | Hemocompatibility and biological activity testing

For hemocompatibility and biological activity testing of coated materials, blood samples from healthy donors who did not take any aspirin or anticoagulant in the last 20 days prior to the experiment were used. Blood was drawn using a 21-gauge needle and citrate vacutainer tubes (BD Biosciences). Platelet-rich plasma (PRP) was prepared by centrifugation of citrate anticoagulated human blood at 100 × g for 15 minutes at room temperature within 60 minutes of collection. Platelet-poor plasma was prepared by 2-step centrifugation at 1500 × g for 15 minutes. The study was approved by the Ethics Committee of the University Hospital of Liège, Liège, Belgium. An informed consent was signed by the donors.

Hemolysis assays were performed in accordance with International Organization for Standardization (ISO) 10993-4 guidance and others [20] upon incubation of coated and noncoated, 8-mm–diameter discs of medical-grade polyurethane (Carbothane 3575A) with a mixture of washed human red blood cells and phosphate-buffered saline (Supplementary Methods). For complement activation assays, coated and noncoated polyurethane discs (0.8 mm) were placed into 0.1% bovine serum albumin-coated wells of 24-well polystyrene plates (Greiner Bio-One CELLSTAR) followed by incubation with 300 μL of citrate anticoagulated whole blood for 60 minutes at 37 °C. Plasma levels of activated complement (C5a) were determined by enzyme-linked immunosorbent assay according to the manufacturer's instructions (R&D Systems). Platelet adhesion on surfaces was analyzed by p-nitrophenyl phosphate photometric assay. PRP was layered on coated and noncoated polystyrene (Greiner Bio-One CELLSTAR multiwell plate) or polyurethane (Carbothane 3575A) surfaces for 60 minutes at 37 °C. For experiments under flow, freshly drawn blood samples were added in the cone and plate device Impact-R system (Matis Medical) before applying a shear rate of 1800/s for 4 minutes. Platelets that adhered to the surface were visualized with an optical microscope and quantified using the Impact-R software, in terms of surface coverage (SC; as percentage) and platelet aggregate size (AS; square micrometer). Single platelet count was measured in collected circulating blood (Cell-Dyn 3700, Abbott Laboratories). Clotting tests were performed using the Stago STart 4 Hemostasis Analyzer and the Nodia nonactivated partial thromboplastin time reagent. For these tests, 120 μL of human plasma (Stago Standard Plasma) prewarmed at 37 °C was added in coated and noncoated wells of a 48-well polystyrene plate (Greiner Bio-One CELLSTAR multiwell plate) and

incubated for 10 minutes at 37 °C. Platelet aggregation experiments were performed with PRP in the presence of ticagrelor-loaded or nonloaded NG solutions (10:1, v:v ratio) under stirring (1200 rpm) at 37 °C using light aggregometry (Chrono-Log Model 700 aggregometer, Kordia).

2.7 | Bacteria adhesion and biofilm formation analysis

Experiments using *S aureus* were conducted in a biosafety level 2 room. One colony of *S aureus* was grown overnight at 37 °C in Tryptic Soy Broth medium under agitation (220 rpm). The bacterial culture was then diluted 100-fold in fresh medium, and bacterial growth was monitored until reaching the exponential growth phase (optical density$_{595}$, 0.5). Ten million colony forming units were incubated for 24 hours at 37 °C in coated or noncoated polystyrene 24-well plates (Greiner Bio-One CELLSTAR multiwell plate). Biofilm mass was analyzed by crystal violet staining.

2.8 | *Ex vivo* valve thrombogenicity testing

Thrombogenicity testing of coated and noncoated Open Pivot mechanical valves was performed in a homemade tester consisting of a pneumatic pump with 2 diaphragms and 35-mm–diameter silicone tubes. Valves were positioned in a silicone ring before filling the system with 600 mL of 2-fold diluted porcine heparinized (Clexane, 3 IU/mL) arterial blood and applying pulsatile flow with a pressure adjusted between 100 and 120 mm Hg for 4 hours. Blood from different pigs was used for each tested valve. Arterial blood was collected under anesthesia from the femoral arteries. The experiments were conducted within 1 hour after blood collection. Blood was analyzed on Cell-Dyn 3700 (Abbott Laboratories) equipped with a veterinary software. Hematological parameters, including platelet count, in each blood sample were in normal range.

2.9 | Pig model of valve implantation

All experiments were conducted in accordance with the European guidelines for animal use in research upon approval by the institutional committee for the ethical use of animals (file #1681). Coated or noncoated, 19-mm–diameter PVs were implanted in the descending thoracic aorta of pigs (Pietrain × Landrace crossbred, weight 110-150 kg) as described in Supplemental Methods. The animals were followed up daily for 1 month. Blood samples were collected before and 2 weeks after the procedure and stored for D-dimers (porcine D-dimer ELISA kit, MyBiosource) and complement C3a (porcine complement 3a, MyBiosource) dosage. After 1 month, valve explantation was realized under general anesthesia (10 mg/kg ketamine, 0.07 mg/kg detomidine, and 0.5 mg/kg midazolam) before proceeding to euthanasia with sodium pentobarbital (intravenous, 140 mg/kg). The explanted valves were washed in NaCl 0.9%. Clots of both sides of the valves were gently detached and weighed. Valve surface was analyzed by scanning electron microscopy, and clots were prepared for transmission electron microscopy analysis, as described in Supplemental Methods.

2.10 | Statistics

Data were reported as mean ± SD or median with IQRs. Normality of the data was assessed using the Shapiro–Wilk test. The Mann–Whitney U-test was used to compare 2 samples. To determine whether differences existed among >2 samples, analysis of variance with post hoc Tukey's test or Kruskal–Wallis with post hoc Dunn's test were used when appropriate. All tests were 2-sided, and a p value of <.05 was considered significant. Statistical analysis was performed using GraphPad Prism 8.2 Software.

3 | RESULTS

3.1 | Bioactive coating development

We used dip coating to deposit successive coating layers. An anchored layer of poly(dopamine) was first formed on the substrate before adding an aqueous solution of PAH, followed by layers of NGs [19] (Supplementary Figure S2). This coating could be attached on metallic surfaces, including gold, pyrolytic carbon, and medical-grade titanium as well as on synthetic polymers, including polystyrene and polyurethane (see below). The coating mechanism involved covalent amine/quinone bonds by Michael addition and/or Schiff base formation between quinones present at the surface of the NGs and amine groups of poly(-allylamine), which led to the formation of a highly stable coating made of cross-linked NGs. PEG was then grafted on top of the NGs by dipping the material in a solution of thiol end-functionalized PEG (Methoxy-PEG-$[CH_2]_2$-SH; weight-average M_w, 2000 or 5000 g/mol). The reaction of the thiol end-group with quinones present at the surface of the NGs provided a strong and covalent anchoring of PEG [19]. In agreement with well-known PEG hydrophilic property [21], the contact angle measured on surface coated with PEG-grafted NGs was equal to 34.11° ± 4.41° (mean ± SD).

Using quartz crystal microbalance coupled with dissipation, we confirmed that all components were successfully deposited according to the selected deposition protocol and redox/pH conditions and remained on the substrate after rinsing with water (Figure 1A).

We then explored the possibility to load NGs with small molecule pharmaceutical agents. To achieve potent antithrombotic activity and prevent device infection, we chose the cyclo-pentyl-triazolo-pyrimidine ticagrelor [22,23], an antiplatelet agent with antibacterial

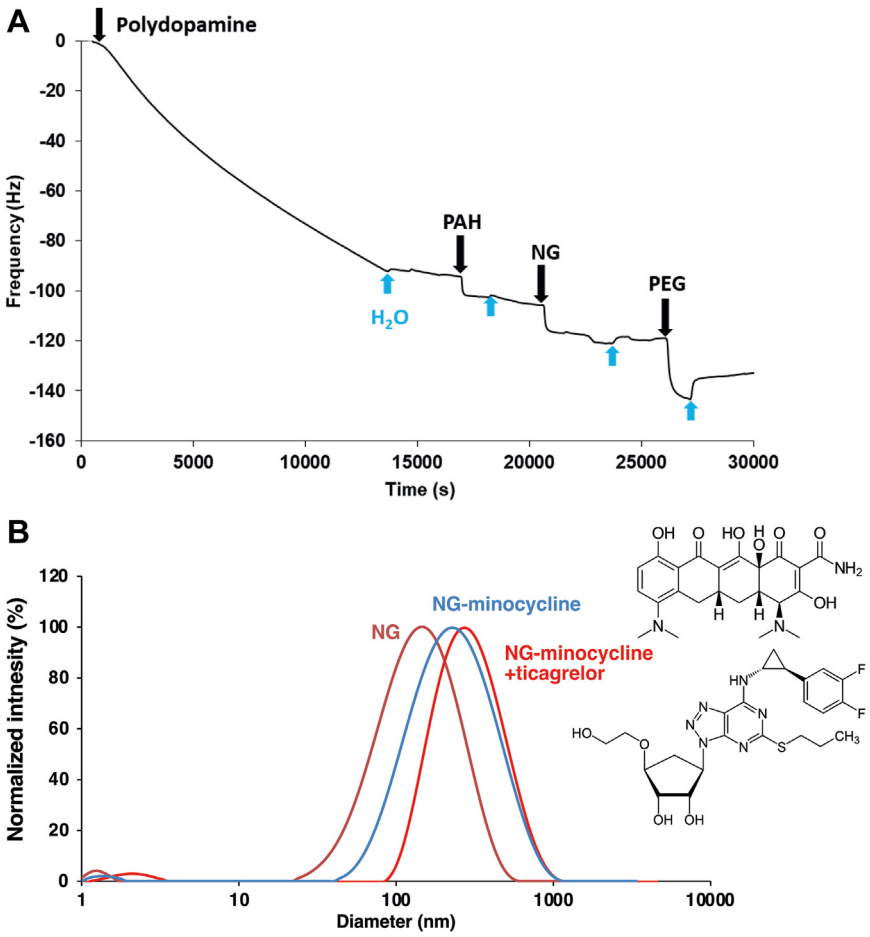

FIGURE 1 Coating chemistry. (A) Real time assessment of multilayer coating build up by quartz crystal microbalance coupled with dissipation. (B) Analysis of nanogel (NG) size and polydispersity by dynamic light scattering. NGs loaded with ticagrelor, ticagrelor plus minocycline and nonloaded NGs are shown. Data are representative of at least 3 independent NG preparations. PAH, poly(allylamine) hydrochloride; PEG, polyethylene glycol.

activity [24–29], and minocycline, a tetracycline antibiotic that has previously been used for preventing bacterial infection in distinct medical device applications [30]. Dynamic light scattering measurement showed NGs with a higher diameter than nonloaded NGs (mean diameter of NGs loaded with ticagrelor, 189.3 ± 5.2 nm; ticagrelor plus minocycline, 272.2 ± 5.7 nm; nonloaded NGs, 119.3 ± 1.9 nm; $n = 3$; $p < .001$), confirming drug incorporation (Figure 1B). The polydispersity index (PI) remained unchanged after NG loading (PI, 0.25 ± 0.02; PI, 0.24 ± 0.01; PI, 0.23 ± 0.03).

3.2 | Coating hemocompatibility and biological activity

Our coating did neither cause hemolysis (Figure 2A) nor complement activation (Supplementary Figure S3). We then tested plasma protein adsorption at the surface of polystyrene wells coated or not with NGs bearing or not PEG of different M_w (M_w, 2000 or 5000 g/mol). We found that PEG grafting conferred plasma protein-repellent property to the coated surface. PEG 5000 significantly inhibited plasma protein adsorption compared with the noncoated surface (Figure 2B). Upon incubation with human PRP, platelet adhesion on NG-coated polystyrene did not differ from that on the noncoated surface (Figure 2C). In this assay, coating grafting with PEG 2000 did not yield increased platelet adhesion on NG-coated surface in contrary to PEG 5000. We next measured contact phase-dependent clotting time in plasma incubated with coated and noncoated materials (Figure 2D). Polystyrene coated with NGs decorated or not by grafted PEG did not induce changes in clotting time, and thus, our coating did not cause coagulation activation. Altogether, these data confirmed the hemocompatibility of the surfaces coated with PEG 2000-grafted NGs.

To mimic the flow conditions of the heart valve environment, we studied shear-induced platelet adhesion and aggregation on polystyrene wells under laminar flow. Material coating with PEG-2000-grafted NGs inhibited platelet adhesion under flow, as shown by reduced percentages of SC by platelets and AS compared with that of noncoated surface (Figure 2E). The decrease in SC on NG-PEG2–coated surface was not associated with a reduction in platelet count in circulating blood (Figure 2E).

We then studied the antiplatelet activity of surfaces coated with ticagrelor-loaded NGs, referred to as nanoreservoirs. To this aim, we first verified that these NGs displayed the expected antiplatelet activity. We determined the minimal concentration of ticagrelor for NG loading required to achieve platelet inhibition. NGs were loaded in the presence of increasing concentrations of ticagrelor before being added to PRP. Platelet aggregation was then induced by

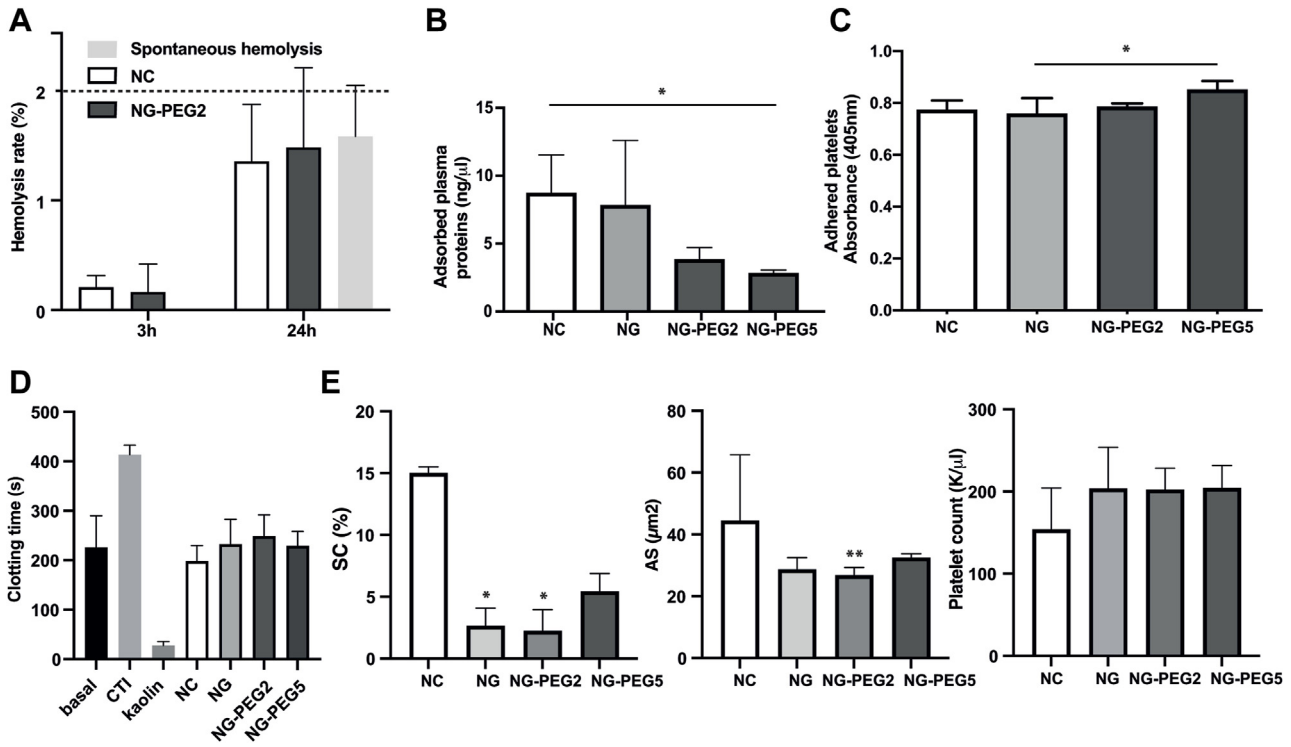

FIGURE 2 Coating hemocompatibility. (A) Polyethylene glycol (PEG)–grafted nanogel (NG) coating is nonhemolytic. Hemolysis rate upon 3- and 24-hour incubation of human washed red blood cells with medical-grade polyurethane discs coated with NGs bearing PEG 2000 (NG-PEG2) or not (NC). Spontaneous hemolysis observed after 24 hours in the absence of any discs is also shown. The dashed line depicts the 2% limit for nonhemolytic materials. Data represent mean ± SD of independent experiments performed on blood samples from 4 healthy donors. (B) Analysis of plasma protein adsorption on polystyrene wells coated with NGs only (NG) or NGs grafted with PEG 2000 (NG-PEG2) or PEG 5000 (NG-PEG5) or left uncoated (NC). Data represent mean ± SD of 4 experiments performed on human plasma from different donors. $^{*}p < .05$, one-way ANOVA with post hoc Tukey's test. (C) Platelet adhesion assay performed on platelet-rich-plasma from 4 different donors. Data represent mean ± SD. $^{*}p < .05$, one-way ANOVA with post hoc Tukey's test. (D) Clotting time measurement in human plasma upon incubation with coated and noncoated polystyrene wells as indicated. Data represent mean ± SD ($n = 4$). Statistical analysis: ANOVA, coated vs noncoated, not significant. (E) Platelet adhesion under flow assessed after 4 minutes. Platelet count in circulating blood is also shown. Data represent median and IQR obtained in 4 independent experiments with blood samples from 4 different donors. $^{*}p < .05$, $^{**}p < .01$ vs NC, Kruskal–Wallis with post hoc Dunn's test. Representative images of stained platelets adhered on the surface after a 4-minute assay. Platelets are aligned with flow direction. AS, aggregate size; CTI, corn trypsin inhibitor; SC, surface coverage.

adenosine diphosphate (ADP) under stirring conditions and recorded over time by light transmission aggregometry. NG-mediated platelet inhibition was compared with the inhibition obtained by directly adding ticagrelor to PRP. Data indicated that using a loading solution of 112 µg/mL ticagrelor during NG formation yielded similar antiplatelet activity as a solution containing 1.8 µg/mL ticagrelor (ticagrelor inhibitory concentration$_{50}$ for *in vitro* inhibition of ADP-induced platelet aggregation, 0.2 µg/mL) [31] (Figure 3A). In a ticagrelor release assay, we further showed progressive drug release from the coated surface (Figure 3B). Moreover, this assay revealed that increasing the number of layers of cross-linked NGs from 1 to 5 significantly augmented the amount of ticagrelor released over time. By high-performance liquid chromatography analysis, we evaluated the total content of releasable drug of coated polyurethane discs to be equal to 10.4 ± 0.9 µg/cm^2 (mean ± SD). NG loading with ticagrelor significantly inhibited platelet accumulation on coated material compared with nonloaded NGs (Supplementary Figure S4).

To protect devices against bacterial infection, we added NGs loaded with minocycline to the coating. We found that a 2 to 3 ratio of minocycline- to ticagrelor-loaded NGs in solution did not interfere with the NG-mediated inhibition of ADP-induced platelet aggregation (Supplementary Figure S5). We observed that a 5-layer assembly of these NGs conferred potent anti *S aureus* biofilm activity to coated surfaces (Figure 3C). We next evaluated the antiplatelet effect of this 5-layer assembly under flow. Since PEG-grafted nonloaded NGs potently inhibited platelet adhesion by themselves under our experimental conditions (Figure 2E), we set up an assay in which human blood was preactivated with ADP. On the noncoated surface, this preactivation step induced the formation of microaggregates in flowing blood, as shown by a drop of single circulating platelets and reduced SC compared with nonactivated conditions (mean platelet count ± SD, 25.6 ± 34.7 vs 144.0 ± 35.6; mean percentage of SC ± SD, 4.8 ± 3.0 vs 15.2 ± 0.4). We found that a 5-layer PEG 2000 grafted ticagrelor and minocycline nanoreservoir coating decreased both SC

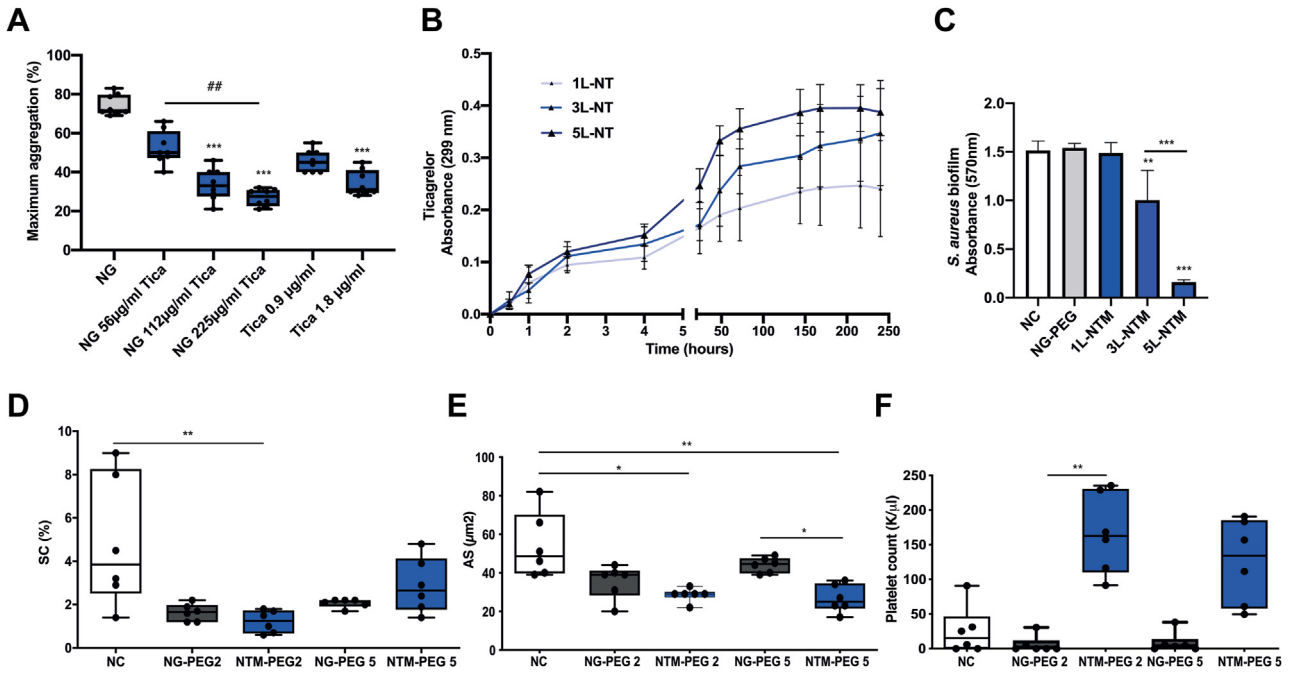

FIGURE 3 Antiplatelet and antibacterial activity of the bioactive coating. (A) Light transmission aggregometry analysis of antiplatelet activity of ticagrelor-loaded nanogels (NGs) in platelet-rich-plasma compared with ticagrelor solution and nonloaded NGs. Platelet aggregation was induced by 10 mM ADP. Box and whisker plots are shown, the horizontal lines representing the median and IQR. Data are from 8 independent experiments performed on platelet-rich-plasma from different donors. $^{***}p < .001$ vs NG, $^{\#\#}p < .01$, Kruskal–Wallis with post hoc Dunn's test. Tica: ticagrelor. (B) Ticagrelor release over time from polyurethane discs coated with 1, 3, or 5 layers of ticagrelor-loaded NGs and polyethylene glycol (PEG) 2000 as top layer (1L-NT, 3L-NT, 5L-NT). Data represent mean ± SD from 3 independent experiments. (C) Analysis of *Staphylococcus aureus* biofilm formation on coated and noncoated PS wells as indicated. Data represent mean ± SD of 4 independent experiments. $^{**}p < .01$, $^{***}p < .001$ vs NC, one-way ANOVA with post hoc Tukey's test. (D, E) Platelet adhesion on various coated surfaces with loaded (NTM) or nonloaded NGs, PEG 2000 (PEG2) or PEG 5000 (PEG5) and noncoated surface (NC) assessed under flow after 4 minutes. Blood was preactivated with ADP (1 µM) for 2 minutes before starting the assay. Box and whisker plots are shown, the horizontal lines representing the median and IQR. Data are from 6 independent experiments performed on blood from different donors. $^{*}p < .05$, $^{**}p < .01$, Kruskal–Wallis with post hoc Dunn's test. (F) Single platelet count measured in circulating blood after the assay. AS, aggregate size; SC, surface coverage.

and AS compared with noncoated surface (Figure 3D, E). The reduction of SC with platelets could not be achieved by grafting PEG 5000 instead of PEG 2000. Using PEG 5000 in addition to nanoreservoirs reduced platelet AS in comparison with nonloaded PEG-grafted coating, but this did not perform better than PEG 2000-containing coating (Figure 3E). In addition, the ADP-induced drop of platelet count was fully restored to normal levels by using the nanoreservoir coating with PEG 2000 but not with PEG 5000 (Figure 3F). Altogether, these data indicate that our nanoreservoir coating bearing PEG 2000 could achieve the intended antithrombotic activity through local ticagrelor release.

3.3 | Coating of mechanical valves, hydrodynamic performance, thromboresistance, and coating durability

Clinically used 19-mm mechanical valves (Open Pivot Bileaflet Heart Valve, Medtronic) were coated as above by dipping in a solution of dopamine, followed by successive dipping in solutions of PAH and a mixture of minocycline- and ticagrelor-loaded NGs (2:3 ratio), and PEG 2000 as a top layer. The hydrodynamic performance of coated mechanical valves in aortic position was verified by using an ISO-compliant left heart model tester (pulse duplicator, VivitroLabs). Regurgitation fraction and effective orifice area were measured under normotensive (70 beats per minute, systolic duration 35%, cardiac output of 5 L/min), hypotensive (45 beats per minute, systolic duration 30%, cardiac output of 5 L/min), and hypertensive (120 beats per minute, systolic duration 50%, cardiac output of 5 L/min) conditions. All measured parameters complied with the ISO 5840 recommendations, and they did not differ from those of noncoated valves (Figure 4). Next, valve thrombogenicity was evaluated in the presence of heparinized pig blood in a homemade tester reproducing pulsatile flow of beating heart (Figure 5). We tested 3 coated and 3 noncoated valves. Macroscopic examination revealed the presence of blood clots on the surface of at least one side of all noncoated valves whereas only 1 coated valve out of 3 showed a small clot on one side of the prosthesis. Scanning electron microscopy analysis further confirmed the presence of platelet- and fibrin-rich thrombi on noncoated valves, whereas the surface of coated valves remained free of thrombi

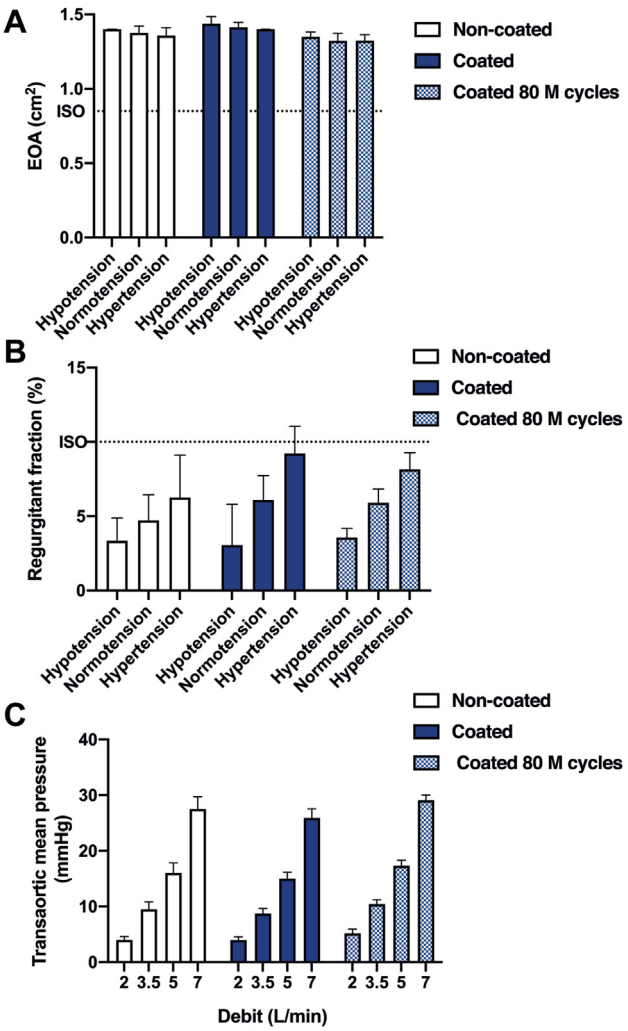

FIGURE 4 Preserved hydrodynamic performance of coated mechanical valves. (A) Valve effective orifice area (EOA). (B) Regurgitant fraction. (C) Transaortic mean pressure. Data represent means ± SD obtained with 4 coated, 2 noncoated Open Pivot mechanical valves by using a pulse duplicator as described in Methods. Two coated valves that were placed in a durability tester for 80 million cycles were also included. Between 3 and 6 measurements per valve were performed. ISO, International Organization for Standardization.

(Supplementary Figure S6). Platelet count measured in blood at the end of the experiments did not differ between coated and noncoated valves. These results underscored the antithrombotic efficacy of our coating on the mechanical valves.

Coating durability was assessed by use of the ISO-compliant HiCycle valve durability tester (VivitroLabs) for 80 million cycles of heart beats, which corresponds to approximately 2 years of human life. Figure 4 shows that valve hydrodynamic performance remained unchanged compared with freshly coated valves. Coating integrity was analyzed by ToF-SIMS combining surface spectroscopy and the depth profile analyses. Spectra in positive and negative mode indicated that the surface chemistry for the 2 coated valves tested after 80 million cycles was kept intact and comparable to freshly coated valve (Supplementary Figure S7). The detection of S^- in negative ion mode on the 3 samples confirmed the presence of grafted PEG-SH on the coated valves. Negative depth profile analysis of C_2H^-, CN^-, C_6H^-, and $C_4H_5O_2^-$ ions indicated that the overall coating assembly remained unchanged. The profiles of $C_2H_3O^-$, $C_2H_3O_2^-$, and $C_4H_5O_2^-$ ions further confirmed intact PEG grafting. Before proceeding to preclinical testing in animals, the same technique was used to assess the resistance of our coating to gamma irradiation sterilization. Coated valves were sterilized by applying a conventional dose of 25 kGy. ToF-SIMS analysis indicated that the overall chemical structure and the thickness of the assembly were both preserved after sterilization (Supplementary Figure S8).

3.4 | *In vivo* preclinical testing

To analyze the antithrombotic efficacy of coated valves *in vivo*, coated or noncoated, 19-mm–diameter PV (Open Pivot Bileaflet Heart Valve, Medtronic) were implanted in the descending thoracic aorta of pigs. The prosthesis was sutured in a 22-mm–diameter 3-cm long vascular graft (Gelsoft Plus gelatin impregnated knitted vascular prosthesis, Terumo), before suturing the graft end-to-end in clamped aortas of heparinized animals (Figure 6A). Pigs were kept nonanticoagulated for 1 month after valve implantation. A total of 9 pigs were implanted with noncoated valves, whereas 4 pigs received a coated prosthesis. During follow-up, none of the pigs showed clinical signs of thromboembolism or of valve dysfunction. We did not detect systemic effects of valve implantation in any of the tested samples. D-dimer levels remained unchanged after valve implantation, and no complement activation was detected (Supplementary Figure S9). Macroscopic analysis of explanted valves revealed much smaller thrombi on the surface of coated valves than on noncoated ones (Figure 6B), which was confirmed by weighing detached clots (Figure 6C). Scanning electron microscopy of the metallic valve surface revealed firmly attached fibrin-rich thrombi on noncoated valves, whereas the coated valves were mainly covered by agglutinated red blood cells (Figure 6D). Histological analysis of clot sections and transmission electron microscopy revealed very dense thrombi on the aortic side (backward) of noncoated valves that were composed of large fibers of cross-linked fibrin in between platelet aggregates and leukocyte infiltrates (Figure 6E). In contrast, clots from both sides of the coated valves displayed features of young red blood cell–rich clots with only few platelets and little thin fibrin fibers (Figure 6E). Overall, these data demonstrate *in vivo* antithrombotic efficacy of our coating.

4 | DISCUSSION

Synthetic polymer coatings have attracted interest in modern medicine to improve biomaterial-related tolerance and performance [32–36]. Self-polymerized catechols, more precisely dopamine, have proven to strongly anchor to different surfaces including metals (eg, Au, Ag, stainless steel) and synthetic polymers (eg, polystyrene,

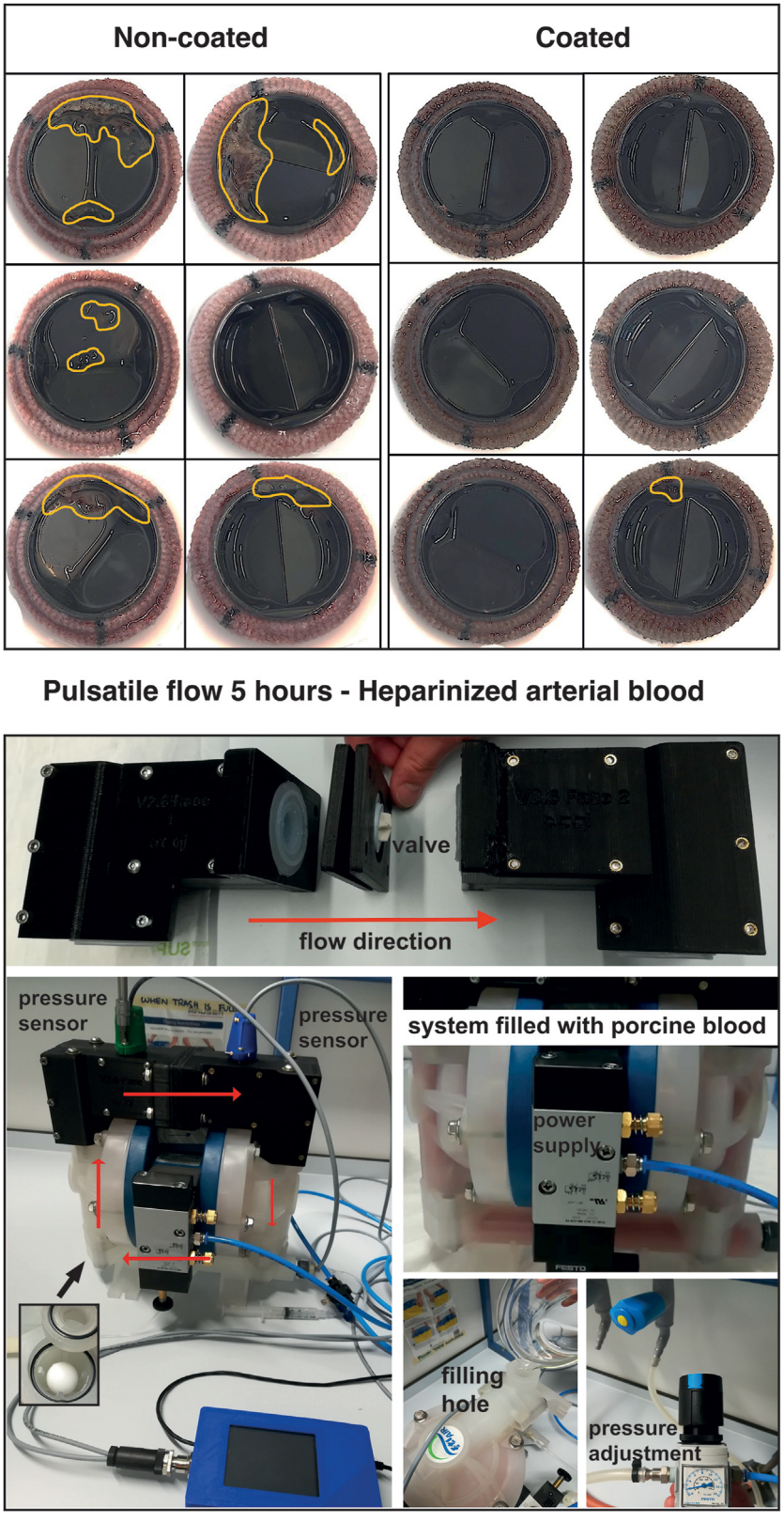

FIGURE 5 *Ex vivo* antithrombotic property of coated mechanical valves. Three Open Pivot mechanical valves coated with 5 layers of ticagrelor and minocycline-loaded nanogels and polyethylene glycol 2000 as top layer and 3 noncoated valves were put in contact of porcine heparinized blood under pulsatile flow conditions for 5 hours in a homemade pulsatile flow tester. Macroscopic surface analysis was performed. Yellow arrows depict thrombi on backward and forward sides of the valves.

polyethylene terephthalate, polyurethanes), making them attractive organic primers for secondary polymer grafting/adhesion [37]. Catechol-based chemistry can also be used for NGs formation by crosslinking a polymethacrylamide containing oxidized catechols (ie, Pox[mDOPA]) with a polyamine (PAH) [19]. However, exploiting the properties of catechols to attach NGs on the surfaces of clinically

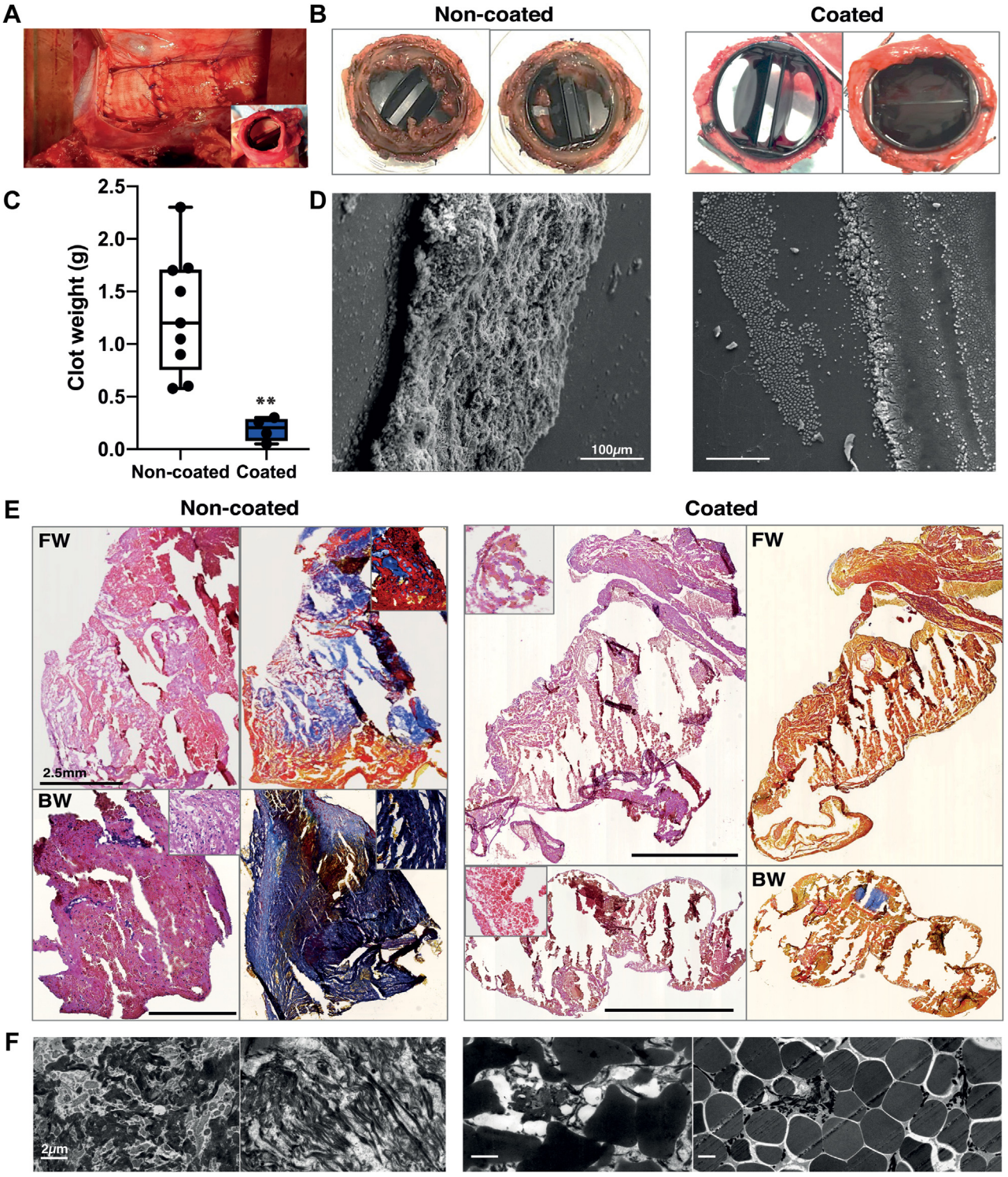

FIGURE 6 *In vivo* antithrombotic property of coated mechanical valves. (A) Coated and noncoated Open Pivot mechanical valves were implanted in the thoracic aorta of nonanticoagulated pigs by use of a vascular graft as described in detail in Methods. (B) Valves were explanted after 1 month. Images are representative of 9 noncoated and 4 coated valves. (C) Total clot weight for coated and noncoated valves. Box and whisker plots are shown, and the horizontal lines representing the median and IQR. $^{**}p < .01$, Mann–Whitney U-test. (D) Scanning electron microscopy analysis of valve surface. (E) Histological analysis of clots detached from coated and noncoated valves. Left panels, hematoxylin eosin staining; right panels, martius scarlet blue staining (yellow: red blood cells, red or purple: fibrin, gray: platelets). Representative images are shown. BW, backward (aortic side); FW, forward (ventricular side). (F) Transmission electron microscopy analysis of clots detached from coated and noncoated valves.

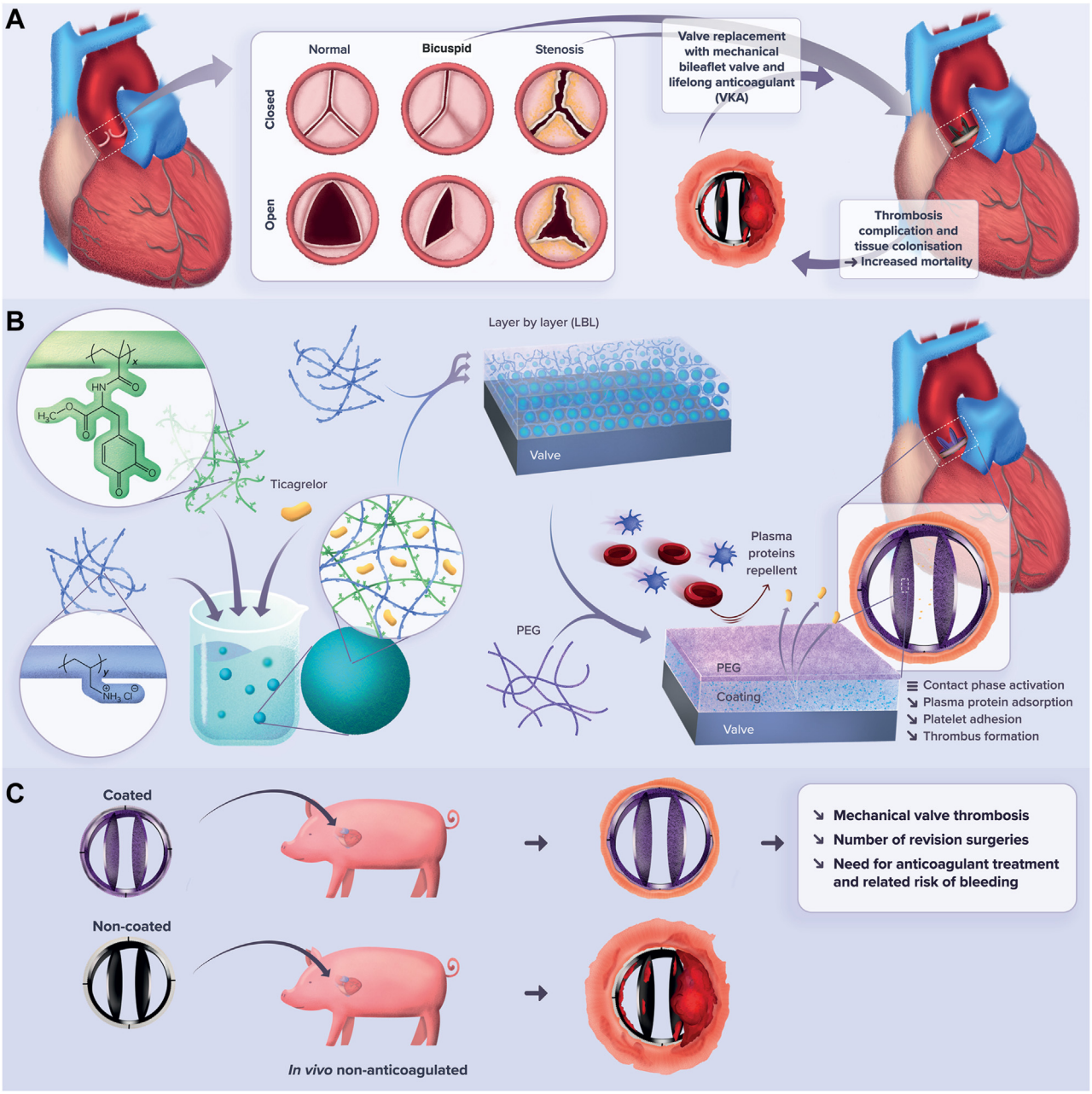

FIGURE 7 Illustration of the bioactive coating approach to prevent thrombotic complications of mechanical heart valves. (A) Valve replacement remains the sole treatment of aortic stenosis. Mechanical valves require lifelong anticoagulation with vitamin K antagonist (VKA) and are still associated with thrombotic complications themselves resulting in high mortality rate. (B) Drug-loaded nanogels are formed by mixing 2 polymers, Pox(mDOPA) and polyallylamine hydrochloride, in the presence of a bioactive compound (ie, ticagrelor). Deposition of nanogels and polyallylamine hydrochloride on valve surface results in a cross-linked multilayer assembly of nanogels. Polyethylene glycol (PEG) grafting on top of the coating produces a valve surface that is repellent for plasma proteins and does not activate coagulation. Locally released ticagrelor prevents platelet accumulation and thrombosis on the valve surface. (C) *In vivo* demonstration of antithrombotic activity of coated valve upon implantation in nonanticoagulated pigs. LBL, layer by layer.

used mechanical PV made of pyrolytic carbon-coated titanium and polyethylene terephthalate is unique. In addition, none of these NGs have ever been designed to encapsulate antithrombotic and antimicrobial agents.

The present innovative coating technology relates to a catechol-based approach to produce a multilayer coating consisting of cross-linked NGs loaded with ticagrelor (antithrombotic) and minocycline (antibiotic) and covalently linked to PEG (Figure 7).

PEG is a neutral, highly hydrophilic, and flexible polymer that has the remarkable ability to prevent protein adsorption thanks to both steric repulsion and chain mobility [38]. PEG has already been used for coating medical devices and proved to be hemocompatible by

reducing material-induced activation of intrinsic coagulation cascade and platelet adhesion [39–41]. Our study confirmed and extended these previous results but also demonstrated that the optimal M_w of PEG to prevent platelet adhesion was 2000 g/mol whereas PEG 5000 g/mol favors some. It has long been known that the more the surfaces are hydrophilic, the more paradoxically they promote platelet activation by reducing the contact angle [42]. Therefore, although PEG 5000 reduced plasma protein adsorption, conversely, it increased platelet adhesion. Moreover, coating comprising PEG 2000 grafted NGs significantly inhibited platelet adhesion under laminar flow.

Ticagrelor (a cyclo-pentyl-triazolo-pyrimidine) is a potent antiplatelet agent (a direct and reversible platelet ADP P2Y12 receptor antagonist) that is widely used in the treatment of acute coronary syndrome [43]. As a first step, we were able to incorporate ticagrelor into the NGs and found that using a loading solution of 112 μg/mL ticagrelor during NG formation produced antiplatelet activity like that of a solution containing 1.8 μg/mL ticagrelor corresponding to approximately 10-fold the IC_{50} of the drug for platelet aggregation inhibition [31]. Moreover, we found that increasing the number of layers of cross-linked NGs from 1 to 5 significantly augmented the amount of ticagrelor released over time.

Similarly, a 5-layer assembly of these NGs in the presence of bacteriostatic antibiotic minocycline also conferred antibiofilm activity to coated surfaces, as assessed *in vitro*. The 5-layer PEG 2000 grafted nanoreservoir also appeared to be the best coating for reducing platelet adhesion when the coated surface is in contact with flowing whole human blood *in vitro*. As such, multilayer assembly of NGs increased the amount of loaded and releasable bioactive molecules.

Mechanical PVs, made from synthetic materials and with unnatural hemodynamics, are prone to thrombus formation without anticoagulant treatment, which increases the risk of bleeding [7]. The discs of clinically used mechanical valves are made of titanium covered with pyrolytic carbon, which is the last revolution in the field of mechanical valves [44].

As an innovative experimental step, we used the developed catechol-based technology to successfully coat all the components of a mechanical bileaflet PV, including its metallic (pyrolytic carbon, titanium) and polymeric (polyethylene terephthalate) constituents, using a dip coating process with solutions of dopamine, PAH, 5 bilayer of PAH and NGs containing minocycline and ticagrelor (2:3 ratio) and PEG 2000 as top layer.

The coating does not alter the hemodynamic performance of a 19-mm mechanical valve, the regurgitation fraction (presence of a backflow), the pressure gradient (presence of a functional stenosis) and the effective orifice area (degree of the disc opening) were not significantly modified regardless of the hemodynamic conditions.

The coated mechanical valves were also less prone to thrombosis when brought into contact with pig blood in a tester replicating the pulsatile flow of the beating heart. The 3 uncoated valves had surface blood clots on at least 1 side, whereas macroscopic examination of the coated valves revealed only a small clot on one side of 1 of the 3 coated valves.

When we talk about medical equipment, durability is at the heart of the debates. This is even more legitimate for a coating. Using a dedicated PV durability tester producing accelerated cardiac cycles, we found that the chemistry of our coating remained unaltered for a period equivalent to 2 years of human life (80 million cycles of heart beats). Also, hydrodynamic performance of the PV, as assessed by the regurgitation fraction, the pressure gradient, and the effective orifice area after 2 years, which represent major data, remained unchanged compared with the freshly coated or uncoated valves.

Another important point is the possibility of sterilizing the coating without altering it. Several methods exist and, here, the use of gamma radiation (25 kGy), the conventional method for mechanical valve sterilization, has proven effective without altering the chemical structure of the coating.

As a final ground-breaking experimental step, the *in vivo* demonstration of our coating hemocompatibility and antithrombotic activity was obtained upon surgical implantation of coated and uncoated mechanical PVs in pigs. Although none of the implanted animals received anticoagulation during the 1-month follow-up, our coating led to impressive reduction of valve thrombosis. The thrombi on the coated valves were smaller, and mostly made up of a few clumped red blood cells with only a few platelets and few thin fibrin fibers (ie, like young clots). Conversely, on the uncoated valves, the thrombi were very compact, firmly fixed, and made up of large, cross-linked fibrin fibers between the platelet aggregates and the leukocyte infiltrates.

In conclusion, the ideal valve substitute should have excellent hemodynamics, long durability, high thromboresistance, and excellent implantability. Unfortunately, this ideal valve substitute does not exist yet, and all the currently available prosthetic mechanical valves have inherent limitations due to their thrombotic and hemorrhagic risks, notwithstanding proper anticoagulation. The present research project led to the development of a revolutionary, innovative, hemocompatible, and unique bioactive coating capable of firmly adhering to mechanical PVs and providing a powerful antithrombotic action while maintaining their hemodynamic performance (Figure 7). Our solution could reduce the need for anticoagulant in patients with mechanical valve, and the number of revision surgeries due to valve thrombosis despite anticoagulation. This new biocoating technology could further be extended to other implantable cardiovascular devices or materials to enhance their long-term performance. Further development will be required to properly assess the industrial transferability of our technology. We need to determine the amount of drug in the coating and how much of it can be released over time. The duration of drug release will depend on the amount of drug loaded in NGs and on the number of NG layers in the coating. However, the optimal drug content will need to be defined for each coating application. In future development of our coating technology for prosthetic heart valves, it will also be useful to include a group where the pigs will be given systemic antithrombotics or anticoagulation to be compared to the local drug release effect.

ACKNOWLEDGMENTS

We thank the GIGA technological platforms and Adeline Deward for creating the illustrations in Figure 7.

AUTHOR CONTRIBUTIONS

P.L., C.D., C.J., A.N., and C.O. conceived the hypothesis and designed the experiments. A.A., L.M., N.J., B.D., M.D., M.T., J.D., A.G., C.S., J.-P.C.-B., and N.S. performed the experiments. P.L., C.O., C.J., and C.D. analyzed the results. P.L. and C.O. wrote the manuscript. P.L., C.O., and C.J. equally supervised this research.

DECLARATION OF COMPETING INTERESTS

C.O., P.L., C.D., and C.J. are inventors on a patent owned by the University of Liège related to medical devices coated with the presented technology (WO2018122318A1).

TWITTER

Cécile Oury @CecileOury

REFERENCES

[1] Writing Committee Members, Otto CM, Nishimura RA, Bonow RO, Carabello BA, Erwin JP III, Gentile F, Jneid H, Krieger EV, Mack M, McLeod C, O'Gara PT, Rigolin VH, Sundt TM III, Thompson A, Toly C. 2020 ACC/AHA Guideline for the management of patients with valvular heart disease: a report of the American College of Cardiology/American Heart Association Joint Committee on Clinical Practice Guidelines. *J Am Coll Cardiol*. 2021;77:e25–197.

[2] Vahanian A, Beyersdorf F, Praz F, Milojevic M, Baldus S, Bauersachs J, Capodanno D, Conradi L, De Bonis M, De Paulis R, Delgado V, Freemantle N, Gilard M, Haugaa KH, Jeppsson A, Jüni P, Pierard L, Prendergast BD, Sádaba JR, Tribouilloy C, et al. 2021 ESC/EACTS Guidelines for the management of valvular heart disease. *Eur Heart J*. 2022;43:561–632.

[3] Frankel WC, Nguyen TC. Artificial heart valves. *JAMA*. 2021;325:2512.

[4] Pibarot P, Dumesnil JG. Prosthetic heart valves: selection of the optimal prosthesis and long-term management. *Circulation*. 2009;119:1034–48.

[5] Chan NC, Weitz JI, Eikelboom JW. Anticoagulation for mechanical heart valves: will oral factor Xa inhibitors be effective? *Arterioscler Thromb Vasc Biol*. 2017;37:743–5.

[6] Alkhouli M, Alqahtani F, Kawsara A, Pislaru S, Schaff HV, Nishimura RA. National trends in mechanical valve replacement in patients aged 50 to 70 years. *J Am Coll Cardiol*. 2020;76:2687–8.

[7] Alkhouli M, Alqahtani F, Simard T, Pislaru S, Schaff HV, Nishimura RA. Predictors of use and outcomes of mechanical valve replacement in the United States (2008-2017). *J Am Heart Assoc*. 2021;10:e019929.

[8] Smith CR, Leon MB, Mack MJ, Miller DC, Moses JW, Svensson LG, Tuzcu EM, Webb JG, Fontana GP, Makkar RR, Williams M, Dewey T, Kapadia S, Babaliaros V, Thourani VH, Corso P, Pichard AD, Bavaria JE, Herrmann HC, Akin JJ, et al. Transcatheter versus surgical aortic-valve replacement in high-risk patients. *N Engl J Med*. 2011;364:2187–98.

[9] Leon MB, Smith CR, Mack MJ, Makkar RR, Svensson LG, Kodali SK, Thourani VH, Tuzcu EM, Miller DC, Herrmann HC, Doshi D, Cohen DJ, Pichard AD, Kapadia S, Dewey T, Babaliaros V, Szeto WY, Williams MR, Kereiakes D, Zajarias A, et al. Transcatheter or surgical aortic-valve replacement in intermediate-risk patients. *N Engl J Med*. 2016;374:1609–20.

[10] Reardon MJ, Van Mieghem NM, Popma JJ, Kleiman NS, Søndergaard L, Mumtaz M, Adams DH, Deeb GM, Maini B, Gada H, Chetcuti S, Gleason T, Heiser J, Lange R, Merhi W, Oh JK, Olsen PS, Piazza N, Williams M, Windecker S, et al. Surgical or transcatheter aortic-valve replacement in intermediate-risk patients. *N Engl J Med*. 2017;376:1321–31.

[11] Mack MJ, Leon MB, Thourani VH, Makkar R, Kodali SK, Russo M, Kapadia SR, Malaisrie SC, Cohen DJ, Pibarot P, Leipsic J, Hahn RT, Blanke P, Williams MR, McCabe JM, Brown DL, Babaliaros V, Goldman S, Szeto WY, Genereux P, et al. Transcatheter aortic-valve replacement with a balloon-expandable valve in low-risk patients. *N Engl J Med*. 2019;380:1695–705.

[12] Kostyunin AE, Yuzhalin AE, Rezvova MA, Ovcharenko EA, Glushkova TV, Kutikhin AG. Degeneration of bioprosthetic heart valves: update 2020. *J Am Heart Assoc*. 2020;9:e018506.

[13] Cahill TJ, Kirtane AJ, Leon M, Kodali SK. Subclinical leaflet thrombosis and anticoagulation after transcatheter aortic valve replacement: a review. *JAMA Cardiol*. 2022;7:866–72.

[14] Makkar RR, Blanke P, Leipsic J, Thourani V, Chakravarty T, Brown D, Trento A, Guyton R, Babaliaros V, Williams M, Jilaihawi H, Kodali S, George I, Lu M, McCabe JM, Friedman J, Smalling R, Wong SC, Yazdani S, Bhatt DL, et al. Subclinical leaflet thrombosis in transcatheter and surgical bioprosthetic valves: PARTNER 3 Cardiac Computed Tomography Substudy. *J Am Coll Cardiol*. 2020;75:3003–15.

[15] Chakravarty T, Søndergaard L, Friedman J, De Backer O, Berman D, Kofoed KF, Jilaihawi H, Shiota T, Abramowitz Y, Jørgensen TH, Rami T, Israr S, Fontana G, de Knegt M, Fuchs A, Lyden P, Trento A, Bhatt DL, Leon MB, Makkar RR, et al. Subclinical leaflet thrombosis in surgical and transcatheter bioprosthetic aortic valves: an observational study. *Lancet*. 2017;389:2383–92.

[16] Patel RP, Price S. Synthesis of benzyl esters of α-amino acids. *J Org Chem*. 1965;30:3575–6.

[17] Charlot A, Sciannaméa V, Lenoir S, Faure E, Jérôme R, Jérôme C, Van De Weerdt C, Martial J, Archambeau C, Willet N, Duwez A-S, Fustine C-A, Detrembleur C. All-in-one strategy for the fabrication of antimicrobial biomimetic films on stainless steel. *J Mater Chem*. 2009;19:4117.

[18] Faure E, Lecomte P, Lenoir S, Vreuls C, Van De Weerdt C, Archambeau C, Martial J, Jérôme C, Duwezd AS, Detrembleur C. Sustainable and bio-inspired chemistry for robust antibacterial activity of stainless steel. *J Mater Chem*. 2011;21:7901.

[19] Faure E, Falentin-Daudré C, Lanero TS, Vreuls C, Zocchi G, Van De Weerdt C, Martial J, Jérôme C, Duwez A-S, Detrembleur C. Functional nanogels as platforms for imparting antibacterial, antibiofilm, and antiadhesion activities to stainless steel. *Adv Funct Mater*. 2012;22:5271–82.

[20] Ovcharenko E, Rezvova M, Nikishau P, Kostjuk S, Glushkova T, Antonova L, Trebushat D, Akentieva T, Shishkova D, Krivikina E, Klyshnikov K, Kudryavtseva Y, Barbarash L. Polyisobutylene-based thermoplastic elastomers for manufacturing polymeric heart valve leaflets: in vitro and in vivo results. *Appl Sci*. 2019;9:4773.

[21] Tseng Y-C, McPherson T, Yuan CS, Park K. Grafting of ethylene glycol-butadiene block copolymers onto dimethyl-dichlorosilane-coated glass by γ-irradiation. *Biomaterials*. 1995;16:963–72.

[22] Springthorpe B, Bailey A, Barton P, Birkinshaw TN, Bonnert RV, Brown RC, Chapman D, Dixon J, Guile SD, Humphries RG, Hunt SF, Ince F, Ingall AH, Kirk IP, Leeson PD, Leff P, Lewis RJ, Martin BP, McGinnity DF, Mortimore MP, et al. From ATP to AZD6140: the discovery of an orally active reversible P2Y12 receptor antagonist for the prevention of thrombosis. *Bioorg Med Chem Lett*. 2007;17:6013–8.

[23] Wallentin L, Becker RC, Budaj A, Cannon CP, Emanuelsson H, Held C, Horrow J, Husted S, James S, Katus H, Mahaffey KW,

Scirica BM, Skene A, Steg PG, Storey RF, Harrington RA, , PLATO Investigators, Freij A, Thorsén M. Ticagrelor versus clopidogrel in patients with acute coronary syndromes. *N Engl J Med*. 2009;361:1045–57.

[24] Sun J, Uchiyama S, Olson J, Morodomi Y, Cornax I, Ando N, Kohno Y, Kyaw MMT, Aguilar B, Haste NM, Kanaji S, Kanaji T, Rose WE, Sakoulas G, Marth JD, Nizet V. Repurposed drugs block toxin-driven platelet clearance by the hepatic Ashwell-Morell receptor to clear Staphylococcus aureus bacteremia. *Sci Transl Med*. 2021;13:eabd6737.

[25] Lupu L, Shepshelovich D, Banai S, Hershkoviz R, Isakov O. Effect of ticagrelor on reducing the risk of gram-positive infections in patients with acute coronary syndrome. *Am J Cardiol*. 2020;130:56–63.

[26] Lancellotti P, Musumeci L, Jacques N, Servais L, Goffin E, Pirotte B, Oury C. Antibacterial activity of ticagrelor in conventional antiplatelet dosages against antibiotic-resistant gram-positive bacteria. *JAMA Cardiol*. 2019;4:596–9.

[27] Lee CH, Lin HW, Lee NY, Lin SH, Li YH. Risk of infectious events in acute myocardial infarction patients treated with ticagrelor or clopidogrel. *Eur J Intern Med*. 2021;85:121–3.

[28] Ulloa ER, Uchiyama S, Gillespie R, Nizet V, Sakoulas G. Ticagrelor increases platelet-mediated Staphylococcus aureus killing, resulting in clearance of bacteremia. *J Infect Dis*. 2021;224:1566–9.

[29] Vicent L, Bruña V, Devesa C, Sousa-Casasnovas I, Juárez M, Alcalá L, Muñoz P, Fernández-Avilés F, Martínez-Sellés M. Ticagrelor and infection risk in patients with coronary artery disease. *Cardiology*. 2021;146:698–704.

[30] Chemaly RF, Sharma PS, Youssef S, Gerber D, Hwu P, Hanmod SS, Jiang Y, Hachem RY, Raad II. The efficacy of catheters coated with minocycline and rifampin in the prevention of catheter-related bacteremia in cancer patients receiving high-dose interleukin-2. *Int J Infect Dis*. 2010;14:e548–52.

[31] Nylander S, Schulz R. Effects of P2Y12 receptor antagonists beyond platelet inhibition—comparison of ticagrelor with thienopyridines. *Br J Pharmacol*. 2016;173:1163–78.

[32] Nandivada H, Villa-Diaz LG, O'Shea KS, Smith GD, Krebsbach PH, Lahann J. Fabrication of synthetic polymer coatings and their use in feeder-free culture of human embryonic stem cells. *Nat Protoc*. 2011;6:1037–43.

[33] Smith JR, Lamprou DA. Polymer coatings for biomedical applications: a review. *Trans IMF*. 2014;92:9–19.

[34] Nathanael AJ, Oh TH. Biopolymer coatings for biomedical applications. *Polymers (Basel)*. 2020;12:3061.

[35] Maan AMC, Hofman AH, Vos WM, Kamperman M. Recent developments and practical feasibility of polymer-based antifouling coatings. *Adv Funct Mater*. 2020;30:2000936.

[36] Mitra D, Kang E-T, Neoh KG. Polymer-based coatings with integrated antifouling and bactericidal properties for targeted biomedical applications. *ACS Appl Polym Mater*. 2021;3:2233–63.

[37] Lee H, Dellatore SM, Miller WM, Messersmith PB. Mussel-inspired surface chemistry for multifunctional coatings. *Science*. 2007;318:426–30.

[38] Alcantar NA, Aydil ES, Israelachvili JN. Polyethylene glycol-coated biocompatible surfaces. *J Biomed Mater Res*. 2000;51:343–51.

[39] Chou SF, Caltrider BA, Azghani A, Neuenschwander PF. Inhibition of platelet adhesion from surface modified polyurethane membranes. *Biomed J Sci Tech Res*. 2020;32:24988–93.

[40] Hutanu D. Recent applications of polyethylene glycols (PEGs) and PEG derivatives. *Mod Chem Appl*. 2014;2:2.

[41] Caló E, Khutoryanskiy VV. Biomedical applications of hydrogels: a review of patents and commercial products. *Eur Polym J*. 2015;65:252–67.

[42] Zhang L, Casey B, Galanakis DK, Marmorat C, Skoog S, Vorvolakos K, Simon M, Rafailovich MH. The influence of surface chemistry on adsorbed fibrinogen conformation, orientation, fiber formation and platelet adhesion. *Acta Biomater*. 2017;54:164–74.

[43] Rodriguez F, Harrington RA. Management of antithrombotic therapy after acute coronary syndromes. *N Engl J Med*. 2021;384:452–60.

[44] More RB. Pyrolytic carbons and the design of mechanical heart valve prostheses. Proceedings of the ASME 2000 International Mechanical Engineering Congress and Exposition. Materials: Book of Abstracts. Orlando, Florida, USA. November 5-10, 2000. pp. 57. ASME.

SUPPLEMENTARY MATERIAL

The online version contains supplementary material available at https://doi.org/10.1016/j.jtha.2023.05.004